

# Synthesis and crystal structure of new organic-based layered perovskites with 2,2'-biimidazolium cations

Zhongjia Tang, Jun Guan and Arnold M. Guloy\*

Department of Chemistry and Texas Center for Superconductivity, University of Houston, Houston, Texas, 77204-5641, USA

Received 23rd June 2000, Accepted 22nd September 2000  
First published as an Advance Article on the web 22nd November 2000

The reaction of 2,2'-biimidazole with metal diiodides,  $\text{PbI}_2$  and  $\text{SnI}_2$ , in hydriodic acid affords new organic-based layered perovskites,  $(\text{C}_6\text{H}_8\text{N}_4)\text{PbI}_4$  and  $(\text{C}_6\text{H}_8\text{N}_4)\text{SnI}_4$ , in which non-primary ammonium organic cations were incorporated with the inorganic layered perovskites. Single crystal X-ray investigations show the aromatic heterocyclic biimidazolium cations form organic layers sandwiched between the metal iodide sheets. The metal iodide perovskite layers exhibit unusual structural features associated with one-dimensional metal halide structures. These structural features are rationalized in terms of stereoactive lone pairs that arise from the weakening of secondary bonds.

## Introduction

The preparation and characterization of tunable organic-inorganic layered perovskites have gained great scientific and technological interest due to their interesting structural,<sup>1</sup> magnetic,<sup>2</sup> electrical,<sup>3</sup> optical,<sup>4</sup> and chemical properties.<sup>5</sup> Possible applications of these layered perovskite materials involve the development of functional materials for novel electronic and optoelectronic devices.<sup>3,4,6,7</sup> Organic-based layered perovskites of  $\text{Pb(II)}$  and  $\text{Sn(II)}$  halides can be regarded as semiconductor/insulator 'natural' quantum wells consisting of inorganic semiconductor layers sandwiched between organic insulator layers.<sup>4,8</sup> In these materials, significant enhancement of exciton binding energies is observed due to dielectric confinement. The dielectric confinement effect of excitons is further amplified in semiconductor/insulator multiple quantum wells when the dielectric constant of the insulator layers is smaller than that of the semiconductor layers.<sup>8</sup> Large exciton binding energies lead to the formation of stable excitons and strong luminescence even at room temperature.<sup>3,4,8</sup>

The layered molecular composite structures are characterized by slabs of multilayer inorganic perovskite sheets alternating with either double layers of organic primary ammonium cations, or layers of organic  $\alpha,\omega$ -diammonium cations. This novel class of crystalline hybrid layered materials exhibit tunable electronic and structural properties through modulation of the inorganic perovskite layers. Incorporating functional organic layers between conducting inorganic sheets adds significant flexibility in modulating the structure and physical properties of the hybrid perovskites. As more complex organic moieties are incorporated into the structure more interesting physical properties may arise from the synergism between the hybrid components.<sup>9</sup> However, the type of organic cations that may be used has been reportedly restricted to primary ammonium ( $\text{R-NH}_3^+$  and  $\alpha,\omega$ -substituted diamines) organic cations.<sup>1,2,7</sup> The reported inability to incorporate non-primary amine cations has led to the conclusion that only organic  $\text{R-NH}_3^+$  moieties are possible.<sup>2a,7</sup> The conclusion was mainly attributed to steric effects and stabilization by weak hydrogen bonding between the organic ammonium cations and the halides of the inorganic perovskite sheets.

Imidazoles represent a class of aromatic molecules that can exist as protonated or deprotonated species while retaining their aromaticity. The potential applications of imidazoles are

amplified when they are incorporated in the dimeric analogue 2,2'-biimidazole.<sup>10</sup> Thus, the biimidazolium dication can potentially behave as an effective two-electron acceptor, whereas the corresponding dianion possesses two bidentate chelating sites.<sup>11</sup>

Herein, we report the syntheses and crystal structures of two new organic-based layered metal halide perovskites with non-primary ammonium cations,  $(\text{C}_6\text{H}_8\text{N}_4)\text{MI}_4$  ( $\text{M} = \text{Pb}, \text{Sn}$ ). These are unprecedented organic-inorganic layered perovskites that feature single layers of biimidazolium cations incorporated between the inorganic  $(\text{MI}_4)^{2-}$  ( $\text{M} = \text{Pb}, \text{Sn}$ ) sheets.

## Experimental

### Synthesis

The title compounds  $(\text{C}_6\text{H}_8\text{N}_4)\text{MI}_4$  ( $\text{M} = \text{Pb}$  **1**,  $\text{Sn}$  **2**) were prepared by reacting the metal diiodides,  $\text{PbI}_2$  (99.999%, Aldrich) and  $\text{SnI}_2$  (99.5%, Aldrich), with 2,2'-biimidazole,  $\text{C}_6\text{H}_8\text{N}_4$ , in hydriodic acid (57%). In the preparation of  $(\text{C}_6\text{H}_8\text{N}_4)\text{PbI}_4$ , the red suspension, formed from the dissolution of stoichiometric amounts of reactants, was heated to 80 °C and acid digested. A high yield (>80%) of  $(\text{C}_6\text{H}_8\text{N}_4)\text{PbI}_4$ , that appeared as red crystals, was obtained after two weeks. Dark-red crystals of  $(\text{C}_6\text{H}_8\text{N}_4)\text{SnI}_4$  were obtained by the slow cooling, from 60 °C to room temperature, of a red hydriodic solution formed from combining stoichiometric amounts of the metal iodide and 2,2'-biimidazole. The title compounds were found to be moderately air-sensitive to a moist atmosphere. Melting points of  $(\text{C}_6\text{H}_8\text{N}_4)\text{PbI}_4$  and  $(\text{C}_6\text{H}_8\text{N}_4)\text{SnI}_4$  were determined and found to be 302 and 300 °C, respectively.

### Crystal structure determination

Single crystals of  $(\text{C}_6\text{H}_8\text{N}_4)\text{PbI}_4$  and  $(\text{C}_6\text{H}_8\text{N}_4)\text{SnI}_4$  were isolated under mineral oil and mounted on glass fibers attached to a goniometer. The goniometer was then moved to the diffractometer cold stream. Diffraction intensities were measured on a Siemens SMART platform diffractometer with a 1 K CCD area detector using  $\text{Mo-K}\alpha$  radiation. A hemisphere of data (1271 frames at 5 cm detector distance) were collected, at 293(2) K, using a narrow-frame method with scan widths of 0.30° in omega an exposure time of 20 s frame<sup>-1</sup> [for  $(\text{C}_6\text{H}_8\text{N}_4)\text{PbI}_4$ ] and 30 s frame<sup>-1</sup> [for  $(\text{C}_6\text{H}_8\text{N}_4)\text{SnI}_4$ ]. The

**Table 1** Crystal data and structure refinement for  $(\text{C}_6\text{H}_8\text{N}_4)\text{PbI}_4$  and  $(\text{C}_6\text{H}_8\text{N}_4)\text{SnI}_4$ 

Compound	1	2
Formula	$(\text{C}_6\text{H}_8\text{N}_4)\text{PbI}_4$	$(\text{C}_6\text{H}_8\text{N}_4)\text{SnI}_4$
$M_w$	850.95	762.45
$T/\text{K}$	293(2)	293(2)
$\lambda/\text{\AA}$	0.71073	0.71073
Crystal system	Monoclinic	Monoclinic
Space group	$C2/c$	$C2/c$
$a/\text{\AA}$	8.7318(7)	8.7238(8)
$b/\text{\AA}$	9.5299(8)	9.5695(9)
$c/\text{\AA}$	19.3682(16)	19.288(2)
$\beta/^\circ$	99.891(1)	100.180(2)
$V/\text{\AA}^3$	1587.7(2)	1584.9(3)
$Z$	4	4
$D_c/\text{Mg m}^{-3}$	3.560	3.195
$\mu/\text{mm}^{-1}$	18.384	9.384
Reflections collected/ independent	3972/1389	3466/1147
$R_{\text{int}}$	0.0495	0.0333
Final $R$ indices	$R1=0.0243$ , $wR2=0.0686$	$R1=0.0231$ , $wR2=0.0543$
$[I>4\sigma(I)]$	$R1=0.0257$ , $wR2=0.0702$	$R1=0.0261$ , $wR2=0.0555$

first 50 frames were re-measured at the end of data collection to monitor instrument and crystal stability, and the maximum correction on  $I$  was  $<1\%$ . The data were integrated using the Siemens SAINT program,<sup>18</sup> with the intensities corrected for Lorentz factors, polarization, air absorption, and absorption due to variation in the path length through the detector faceplate. A psi-scan [on  $(\text{C}_6\text{H}_8\text{N}_4)\text{PbI}_4$ ] and SADABS<sup>19</sup> [on  $(\text{C}_6\text{H}_8\text{N}_4)\text{SnI}_4$ ] absorption corrections were applied based on the entire data sets. Redundant reflections were averaged. Final cell constants were refined using 3709 reflections having  $I>10\sigma(I)$  for  $[(\text{C}_6\text{H}_8\text{N}_4)\text{PbI}_4]$ , and using 4086 reflections having  $I>10\sigma(I)$  for  $[(\text{C}_6\text{H}_8\text{N}_4)\text{SnI}_4]$ . The two structures were solved by direct methods and refined by full-matrix least-squares calculations on  $F^2$ . All calculations were made with use of the Siemens SHELXTL package.<sup>20</sup> The Laue symmetry was determined to be  $2/m$ , and from the systematic absences noted the space group was shown to be either  $Cc$  or  $C2/c$  for  $(\text{C}_6\text{H}_8\text{N}_4)\text{PbI}_4$  and  $(\text{C}_6\text{H}_8\text{N}_4)\text{SnI}_4$ . Hydrogen atoms attached to N were located from a difference map, and refined independently for  $(\text{C}_6\text{H}_8\text{N}_4)\text{PbI}_4$ .

Results of the single crystal X-ray investigations are summarized in Table 1. Selected bond distances and angles for  $(\text{C}_6\text{H}_8\text{N}_4)\text{PbI}_4$  and  $(\text{C}_6\text{H}_8\text{N}_4)\text{SnI}_4$  are listed in Table 2. CCDC reference number 1145/249. See <http://www.rsc.org/suppdata/jm/b0/b007639m/> for crystallographic files in .cif format.

## Results and discussion

The isostructural compounds,  $(\text{C}_6\text{H}_8\text{N}_4)\text{PbI}_4$  and  $(\text{C}_6\text{H}_8\text{N}_4)\text{SnI}_4$ , both belong to the monoclinic crystal system, crystallizing in space group  $C2/c$  (no. 15). The asymmetric unit consists of half units of the  $(\text{MI}_4)^{2-}$  unit (a part of one layer of corner-shared octahedra) and 2,2'-biimidazole,  $(\text{C}_6\text{H}_8\text{N}_4)^{2+}$  cation. The unit cell of  $(\text{C}_6\text{H}_8\text{N}_4)\text{PbI}_4$  and  $(\text{C}_6\text{H}_8\text{N}_4)\text{SnI}_4$  consists of a two-dimensional inorganic anion  $(\text{MI}_2\text{I}_{4/2})^{2-}$  — a mono-layered perovskite sheet, and 2,2'-biimidazolium cations packed between the inorganic layers, as shown in Fig. 1.

The structural differences between the structures of  $(\text{C}_6\text{H}_8\text{N}_4)\text{PbI}_4$  and  $(\text{C}_6\text{H}_8\text{N}_4)\text{SnI}_4$  arise from the degree of distortion from ideal octahedral geometry of the  $\text{MI}_6$  unit, as shown in Fig. 2. The  $\text{PbI}_6$  unit in  $(\text{C}_6\text{H}_8\text{N}_4)\text{PbI}_4$  is a distorted octahedron wherein the Pb–I distances are asymmetric; equatorial bonds are 3.1045(5) and 3.3679(5) Å. The terminal apical Pb–I bonds are 3.2179(5) Å. The resulting I–Pb–I *trans*

**Table 2** Selected bond lengths (Å) and angles ( $^\circ$ ) for  $(\text{C}_6\text{H}_8\text{N}_4)\text{PbI}_4$  and  $(\text{C}_6\text{H}_8\text{N}_4)\text{SnI}_4$ 

	$(\text{C}_6\text{H}_8\text{N}_4)\text{PbI}_4$	$(\text{C}_6\text{H}_8\text{N}_4)\text{SnI}_4$
M–I ( $2 \times$ )	3.1045(5)	2.9328(6)
M–I ( $2 \times$ )	3.3679(5)	3.5580(6)
M–I <sub>apical</sub> ( $2 \times$ )	3.2179(5)	3.1900(4)
I–M–I	90.592(19)	93.44(2)
I–M–I	94.834(17)	94.54(2)
I–M–I	79.942(17)	77.55(2)
I–M–I <sub>apical</sub>	87.700(12)	89.17(1)
I–M–I <sub>apical</sub>	94.242(12)	93.89(1)
I–M–I <sub>apical</sub>	88.680(11)	88.01(1)
I–M–I <sub>apical</sub>	89.207(12)	88.52(1)
I–M–I	173.687(17)	171.83(2)
I <sub>apical</sub> –M–I <sub>apical</sub>	177.244(16)	175.55(2)
M–I–M	173.687(17)	171.83(2)

bond angles are 174 and 177 $^\circ$  for equatorial and apical Pb–I bonds, respectively. In other mono-layered Pb(II) and Sn(II) iodide perovskites, with alkylammonium cations, the analogous bond distances are close to having symmetric values and the *trans* bond angles are essentially 180 $^\circ$ .<sup>7,12–14</sup> Hence, the observed distortions from ideal octahedral geometry indicate an onset of a stereoactive lone pair.

The  $\text{SnI}_6$  unit in  $(\text{C}_6\text{H}_8\text{N}_4)\text{SnI}_4$  also feature three pairs of Sn–I distances: terminal axial bonds of 3.1900(4) Å, equatorial bonds of 2.9328(6) and 3.558(1) Å. The observed distortion from octahedral geometry is again illustrated by the bond asymmetry of the *trans* Sn–I distances at the equatorial positions. The values observed in  $(\text{C}_6\text{H}_8\text{N}_4)\text{SnI}_4$  represent the largest bond difference between *trans* bonds in any other layered metal halide perovskite. Similar asymmetries in Sn(II) halides, previously observed in chain derivatives of the mono-layer  $\text{SnI}_4$  perovskites, were reportedly attributed to stereoactive lone pairs.<sup>15</sup> It is further important to note that the stereochemical activity of lone pairs in the organic–inorganic perovskites of Sn and Pb halides normally arise in one-dimensional systems of  $\text{MI}_6$  octahedra, as in Pb(II) and Sn(II) halide chains.<sup>13,15</sup> Moreover, it is generally observed that Sn(II) compounds exhibit a larger degree of stereoactive lone pairs than their Pb(II) analogs.

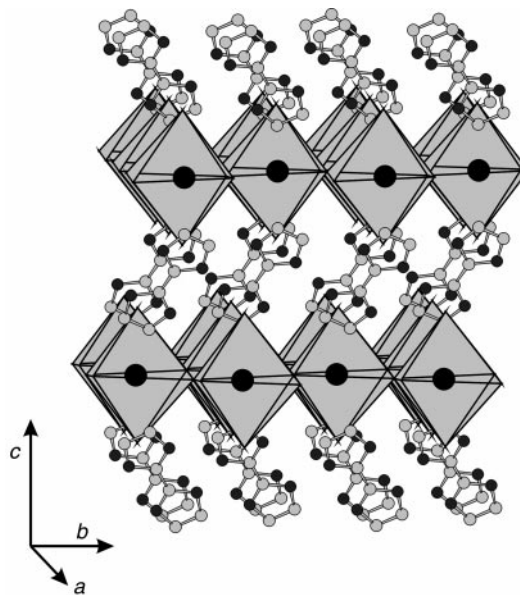


**Fig. 1** A polyhedral representation of the unit cell of the crystal structure of  $(\text{C}_6\text{H}_8\text{N}_4)\text{PbI}_4$ . The crystal structure of  $(\text{C}_6\text{H}_8\text{N}_4)\text{SnI}_4$  is very similar with slight differences in the M–I distances and I–N–I angles. Carbon and nitrogen atoms are represented as grey and black spheres, respectively.

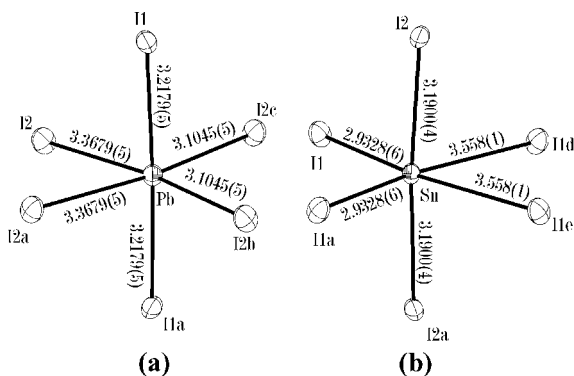


**Fig. 2** ORTEP representation of the  $MI_6$  octahedral units in compounds (a)  $(C_6H_8N_4)PbI_4$ , and (b)  $(C_6H_8N_4)SnI_4$ . The M–I bond distances (Å) are indicated. Ellipsoids are drawn at 50% probability.

In both compounds, the metal atoms are displaced from the centers of octahedra, with Sn atoms in  $(C_6H_8N_4)SnI_4$  exhibiting a larger displacement (0.317 Å) than Pb (0.13 Å). The effect of the stereoactive lone pair, observed more significantly in  $(C_6H_8N_4)SnI_4$ , can be related to the weakening of the secondary bonds in the inorganic  $(MI_4)^{2-}$  perovskite layers. This is manifested by the lengthening of equatorial M–I distances and the concomitant decrease of its M–I *trans* bond. The effect of the active lone pair is further manifested by an ‘axial compression’ of the  $SnI_6$  octahedra in  $(C_6H_8N_4)SnI_4$  ( $I_{\text{apical}}/I_{\text{equatorial}}=0.983$ ) relative to the  $SnI_6$  octahedra in analogous alkylammonium tin(II) layered perovskites.<sup>7,12–14</sup>

The 2,2′-biimidazolium  $(C_6H_8N_4)^{2+}$  cations in the organic layers have the expected geometry associated with doubly protonated dicationic species. Moreover, the 2,2′-biimidazolium cation, which may also act as a two-electron acceptor, is conjugated and the  $\pi$ -electrons are delocalized over the entire molecule. This is in contrast to all previously reported organic–inorganic layered perovskites that form with primary amines having saturated and unsaturated side chains. Previously reported layered organic–inorganic perovskites having  $\pi$ -ring systems have at least one  $CH_2$  unit and an ammonium group between the organic  $\pi$ -system and the inorganic layers.<sup>1,2,7,16</sup> Another interesting feature in the structures of  $(C_6H_8N_4)PbI_4$  and  $(C_6H_8N_4)SnI_4$  is the penetration of the aromatic rings of the cation well into the perovskite ‘bay region’ formed by the apical iodides. The penetration results in the terminal axial iodides nominally capping the five-member imidazolium ring of the cation. This is the closest approach reported between iodide ions of layered perovskite metal halides with an aromatic ring of the organic layer. The planar  $(C_6H_8N_4)^{2+}$  dications, tilted with respect to the *c*-axis, are parallel with neighboring cations and the resulting organic layers stack alternately with  $(PbI_4)^{2-}$  layers.

Aside from the irregularity of the  $MI_6$  octahedra due to active lone pairs, and the significant decrease in secondary bonding, another significant difference between primary alkylammonium layered perovskites and the title compounds is the overall orientation of the inorganic perovskite layers. The layered inorganic structures of  $(C_6H_8N_4)PbI_4$  and  $(C_6H_8N_4)SnI_4$  are unusually ‘flatter’ than the ‘buckled’ or ‘corrugated’ layers of the  $R-NH_3$  perovskites.<sup>7,12,13</sup> The ‘corrugation’ of the perovskite layers in the alkylammonium compounds is associated with the angular distortion or ‘twisting’ of the  $MI_6$  octahedra within the inorganic metal halide sheets.<sup>7</sup> The ‘twisting’ distortion of the inorganic layer was attributed to the presence of significant hydrogen bonding between the iodides of the layers and the ammonium moieties of the cations.<sup>1,2,7</sup> Hence, the distortion can be correlated with the M–I–M angles around the bridging halide of the perovskite slab. The M–I–M angles in  $(C_6H_8N_4)PbI_4$  and  $(C_6H_8N_4)SnI_4$  are nearly linear with values of 174 and 172°, respectively. In

$R-NH_3$  layered perovskites the M–I–M angles reportedly range from 140 to 160°. <sup>12,13,17</sup> Hence, the ‘flatness’ of the metal iodide perovskite layers correlates well with the overall significance and strength of the H-bonding interaction between the inorganic and organic components.<sup>17</sup>

The significance of hydrogen bonding can also be assessed by the orientation of the cations with respect to the apical iodides, as shown in Fig. 3. The N–I distances between the cations and the terminal iodides are 3.534(1) and 3.574(1) Å, with the pairs of N atoms on each imidazole ring close to adjacent inorganic layers. It can be maintained that the inorganic layers are linked to the adjacent layers by the cations through weak hydrogen bonding. However, these interactions are significantly weaker than those alluded to in the alkylammonium layered perovskites.<sup>1,2,7</sup> Hence, it may be argued that the weakening of the H-bonding between the anionic layers and the organic cations may be related to the weakening of the secondary bonds in the inorganic layer. Further investigations on the effects of noncovalent interactions and secondary bonding in these hybrid materials are currently in progress.

### Concluding remarks

In this paper, we have described the preparation and crystal structures of two new layered organic-based perovskites having non-primary ammonium organic cations incorporated within the layered metal iodides. The metal iodide perovskite layers exhibit unusual structural features manifested by significant distortions from the usual octahedral units found in previously reported layered perovskites. The unusual structures of  $(C_6H_8N_4)PbI_4$  and  $(C_6H_8N_4)SnI_4$  emphasize the significant and crucial effects of secondary bonding and non-covalent interactions between organic and inorganic moieties in the supramolecular structure of organic–inorganic layered perovskites. The stability, orientation and termination, and the structural details of layered perovskite structures can be finely tuned by addressing important noncovalent organic–inorganic interactions. These provide additional fine variables in tuning the structure and electronic properties of layered organic–inorganic perovskites.

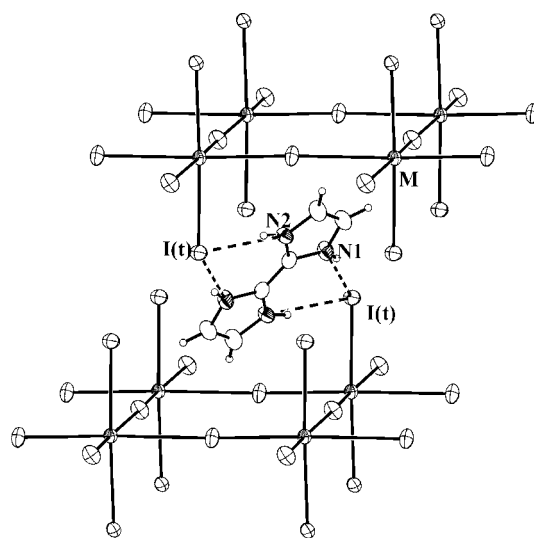


**Fig. 3** ORTEP representation of the packing of 2,2′-biimidazolium ions between two  $(MI_4)^{2-}$  layers in  $(C_6H_8N_4)PbI_4$  and  $(C_6H_8N_4)SnI_4$ . Dashed lines represent closest distances between N and I atoms. M = Pb:  $I(t)-N(1)=3.550(1)$  Å,  $I(t)-N(2)=3.562(1)$  Å; M = Sn:  $I(t)-N(1)=3.534(1)$  Å,  $I(t)-N(2)=3.574(1)$  Å. Ellipsoids are drawn at 50% probability.

## Acknowledgements

This work was supported in part by the Robert A. Welch Foundation, the State of Texas through the Texas Center for Superconductivity, and MRSEC Program of the National Science Foundation under Award Number DMR-9632667. We thank Prof. R. Thummel for the gift of 2,2'-biimidazole used in the syntheses.

## References

- (a) D. B. Mitzi, C. A. Feild, W. T. A. Harrison and A. M. Guloy, *Nature*, 1994, **369**, 467; (b) U. Walther, D. Brinkmann, G. Chapuis and H. Arend, *Solid State Commun.*, 1978, **27**, 901; (c) H. Arend, W. Huber, H. Mischgofsky and G. K. Richter-Van Leeuwen, *J. Cryst. Growth*, 1978, **43**, 213; (d) G. F. Needham, R. D. Willet and H. F. Franzen, *J. Phys. Chem.*, 1984, **88**, 674.
- (a) P. Day, *Philos. Trans. R. Soc. London, Ser. A*, 1985, **314**, 145; (b) L. J. de Jongh and A. R. Miedema, *Adv. Phys.*, 1974, **23**, 1; (c) G. V. Rubenacker, D. N. Haines, J. E. Drumheller and K. Emerson, *J. Magn. Magn. Mater.*, 1984, **43**, 238.
- (a) D. B. Mitzi, S. Wang, C. A. Feild, C. A. Chess and A. M. Guloy, *Science*, 1995, **267**, 1473; (b) M. F. Mostafa, M. M. Abdel-Kader, S. S. Arafat and E. M. Kandeel, *Phys. Scr.*, 1991, **43**, 627; (c) G. C. Papavassiliou, I. B. Koutselas, A. Terzis and M. H. Whangbo, *Solid State Commun.*, 1994, **91**, 695.
- (a) T. Ishihara, J. Takahashi and T. Goto, *Phys. Rev. B*, 1990, **42**, 11099; (b) J. Calabrese, N. L. Jones, R. L. Harlow, D. Thorn and Y. Wang, *J. Am. Chem. Soc.*, 1991, **113**, 2328; (c) G. C. Papavassiliou, *Prog. Solid State Chem.*, 1997, **25**, 125.
- (a) B. Tieke and G. Wegner, *Angew. Chem., Int. Ed. Engl.*, 1984, **20**, 687; (b) B. Tieke and G. Chapuis, in *Crystallographically Ordered Polymers*, ed. M. J. Comstock, ACS Symposium Series, 337, ACS, Washington DC, 1987, pp. 61–78.
- (a) C. R. Kagan, D. B. Mitzi and C. D. Dimitrakopoulos, *Science*, 1999, **286**, 945; (b) M. Era, S. Morimoto, T. Tsutsui and S. Saito, *Synth. Met.*, 1995, **71**, 2013.
- D. B. Mitzi, *Prog. Inorg. Chem.*, 1999, **48**, 1.
- (a) M. Era, T. Morimoto, T. Tsutsui and S. Saito, *Appl. Phys. Lett.*, 1994, **65**, 676; (b) E. A. Muljarov, S. G. Tikhodeev, N. A. Gippius and T. Ishihara, *Phys. Rev. B: Condens. Matter*, 1995, **51**, 14370.
- L. Ouahab, *Chem. Mater.*, 1997, **9**, 1909.
- (a) R. P. Thummel, V. Goulle and B. Chen, *J. Org. Chem.*, 1989, **54**, 3057; (b) R. P. Thummel, F. Lefoulon and R. Mahadevan, *J. Org. Chem.*, 1985, **50**, 3824.
- (a) S. W. Kaiser, R. B. Saillant, W. M. Butler and P. G. Rasmussen, *Inorg. Chem.*, 1976, **15**, 2681; (b) R. Usen, J. Gimeno, J. Fornies and F. Martinez, *Inorg. Chim. Acta*, 1981, **50**, 173; (c) V. W. Beck, F. Gotzfried and M. Riederer, *Z. Anorg. Allg. Chem.*, 1976, **423**, 97.
- D. B. Mitzi, *Chem. Mater.*, 1996, **8**, 791.
- J. Guan, Z. Tang and A. M. Guloy, *Chem. Commun.*, 1999, 1833.
- J. Guan, Ph.D. thesis, University of Houston, USA, 2001.
- S. Wang, D. B. Mitzi, C. A. Field and A. M. Guloy, *J. Am. Chem. Soc.*, 1995, **117**, 5297.
- V. Chakravarthy and A. M. Guloy, *Chem. Commun.*, 1997, 697.
- J. del Hoyo, MSc. thesis, University of Houston, USA, 1997.
- SAINT, Program for area detector absorption correction, Siemens Analytical X-Ray Instruments Inc., Madison, WI, USA, 1994–1996.
- G. M. Sheldrick, Program for area detector absorption correction, Institut für Anorganische Chemie, Universität Göttingen, Göttingen, 1996.
- G. M. Sheldrick, SHELXTL, An integrated system for solving, refining and displaying crystal structures from diffraction data (revision 5.1), Institut für Anorganische Chemie, Universität Göttingen, Göttingen, 1985.
- M. N. Burnett and C. K. Johnson, ORTEP3, Report ORNL-6895, Oak Ridge National Laboratory, Oak Ridge, TN, 1996.